# A Localizing Basis Functions Representation for Low–Low Mode SST and Gravity Gradients Observations

W. Keller
Institute of Geodesy, Universität Stuttgart, Geschwister-Scholl-Str. 24D, D-70174 Stuttgart, Germany

**Abstract.** For geophysical/ oceanographic/ hydrological applications of dedicated gravity field missions regional gravity field solutions are of higher interest than the usual global solutions. In order to derive regional solutions, so-called in-situ observations like line-of-sight accelerations or satellite gradiometry data are optimal, since they do not change, if the potential outside a infinitesimal neighborhood of the observation point changes. Therefore, in-situ observations do not introduce influences from outside the region under consideration. The localization on the observation-side has to be balaced by a localization on the model-side.

The usual spherical harmonics representation is not appropriate for the desired regional solution, because spherical harmonics have a global support. In order to model local phenomena by base functions with a global support, the superposition of a large number of those global base functions is necessary.

For this reason the paper aims at an establishment of a direct relationship between several types of in-situ observations and the unknown coefficients of a localizing basis functions representation of the regional gravity field.

**Keywords.** Satellite-to-satellite tracking, localizing base functions, representation of rotation group, Wigner functions

## 1 Introduction

The temporal data-sampling of the Earth's gravity field by an orbiting satellite is transformed via the orbital movement of the satellite and the rotation of the Earth into a spatial sampling on the surface of a sphere. In general the resulting data-spacing on the Earth is non-uniform and coarser than the theoretical resolution limit, stemming from the temporal data sampling. The usual technique for the analysis of dedicated gravity field satellite missions is the the representation of the resulting gravity field solution as a series expansion in spherical harmonics. Due to the fact that the related surface spherical harmonics have a global support on the unit sphere and the data sampling is non-uniform, the theoretical resolution limit, deduced from the temporal data sampling rate, cannot be reached and the spherical harmonics solution includes a certain smoothing of details in the gravity field. This becomes obvious when the original observations are compared with synthetic observation, computed from an existing gravity field solution. In Figure 1 the difference between the original GRACE range-rates and the synthetic range-rates computed from the GRACE gravity field solution GGSM02 is plotted. It is clearly visible that the difference is not white noise but contains a residual signal. This residual signal is caused by the fact that, due to their global support and due to the given data-distribution, spherical harmonics are not able to capture all signal details. In order to capture also the residual signal components, two measures have to be taken

1. Representation of the residual (so far not captured gravity field) by localizing basis functions in the region under consideration.
2. Usage of so-called in-situ observation, as e.g. line-of-sight accelerations or satellite gradiometry data, for sensing of the residual field, to make sure that no influences from outside the region under consideration enter the observations.

In Keller and Sharifi (2005) it was shown that with proper reductions low–low mode SST observations can be treated as along-track gravity gradients. Therefore, the results to be presented here for gravity gradients do implicitly also hold for low–low mode SST observations.

So far the only in-situ observation with a clear relationship to the unknown parameters of a localizing basis function representation are the radial gravity tensor components observations (cf. Freeden et al. (1999)). To the author's knowledge no

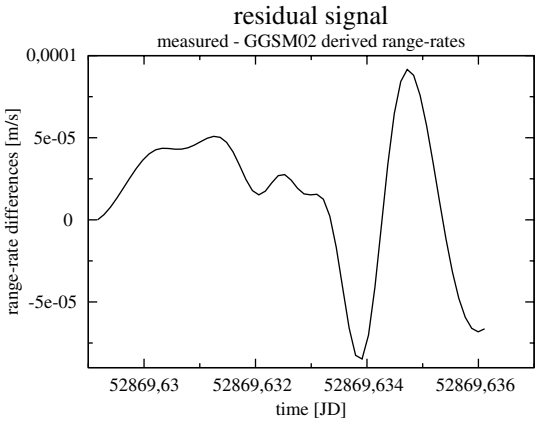


**Fig. 1.** Difference between original range-rates and synthetic range-rates of GRACE along a 10 min arc.

other gravity-field related observations have been expressed in a simple analytic form as functionals on localizing base functions in geodetic literature so far. The paper aims at an establishment of simple relationships also for the along-track and the out-of-plane gravity tensor components.

## 2 State-of-the-Art

Gravity field modeling by localizing base functions means to approximate the unknown potential $V$ by a linear combination of special base functions:

$$V(\mathbf{x}) = \sum_i c_i \psi_i(\mathbf{x}). \tag{1}$$

Here the base functions $\psi_i$ are localizing base functions having the following structure

$$\psi_i(\mathbf{x}) := \psi(g_i^{-1}\mathbf{x}), \quad g_i \in SO(3) \tag{2}$$

and

$$\psi(\mathbf{x}) = \sum_{n\in\mathbb{N}} \sigma_n^2 P_n(\mathbf{e}_3 \cdot \frac{\mathbf{x}}{\|\mathbf{x}\|}) \tag{3}$$

where $P_n$ are the Legendre-polynomials and $\mathbf{e}_3$ is a unit-vector pointing in the direction of 3rd axis of the underlying cartesian coordinate system. The sequence $\{\sigma_n\}$ controls the decay of the base function $\psi$. The generic base function $\psi$ is located at the north-pole of the sphere and the actual base functions are the rotated copies of this generic function.

So far the only well-established method to relate in-situ observations to a localizing base function representation of the field is an approach which could be called *spectral modeling*.

### Spectral Modeling

Spectral modeling can be applied in those cases, where the gravity field-related observation can be represented by a so called *invariant pseudo-differential operator* (PDO) $p$ on $C^\infty(\sigma_r)$, the space of all infinite often differentiable functions on a sphere of radius $r$. A PDO is called invariant, if it is invariant against rotations $g$ out of $SO(3)$

$$[pu](g^{-1}\mathbf{x}) = p[u(g^{-1}\mathbf{x})].$$

This leads to the consequence, that all surface spherical harmonics $Y_{n,m}$ of the same degree $n$ are eigenfunctions belonging to the same eigenvalue $p \wedge (n)$

$$pY_{n,m}(\frac{\omega}{r}) = p \wedge (n) \cdot Y_{n,m}(\frac{\omega}{r}). \tag{4}$$

The eigenvalues $p \wedge (n)$ are called the *spherical symbols* of the PDO $p$.

Examples for invariant PDOs are the radial derivatives and the Poisson operator $P_R^r$ for harmonic upward continuation:

| $p$ | $p \wedge (n)$ |
|---|---|
| $P_R^r$ | $\left(\frac{R}{r}\right)^{n+1}$ |
| $\partial u/\partial r$ | $-\frac{n+1}{r}$ |
| $\partial^2 u/\partial r^2$ | $\frac{(n+1)(n+2)}{r^2}$ |

From the *addition theorem*

$$\frac{2n+1}{2} P_n(\zeta\cdot\eta) = \sum_{m=-n}^{n} Y_{n,m}(\zeta) Y_{n,m}^*(\eta), \quad \zeta,\eta \in \sigma_1 \tag{5}$$

for each invariant PDO $p$ immediately follows

$$p\psi_i(\mathbf{x}) = \psi_i^p(\mathbf{x}) \tag{6}$$

$$\psi^p(\mathbf{x}) := \sum_{n\in\mathbb{N}} \left(\sigma_n^2 \cdot p \wedge (n)\right) P_n(\mathbf{e}_3 \cdot \frac{\mathbf{x}}{\|\mathbf{x}\|}) \tag{7}$$

Hence the application of an invariant PDO on a base function results in a change of its decay. The spectral modeling assumes that a certain quantity $\Gamma \in C^\infty(\sigma_r)$ is given on the sphere $\sigma_r$ , which is the image of a unknown function $u \in C^\infty(\sigma_R)$ under the invariant PDO $p$

$$\Gamma = pu. \tag{8}$$

Both the given data $\Gamma$ and the unknown function $u$ can be represented as linear combinations of systems of localizing base functions $\psi_i^p$ and $\psi_i$, respectively.

$$\Gamma = \sum_i c_i \psi_i^p, \quad u = \sum_i d_i \psi_i, \tag{9}$$

with the known coefficients $d_i$ and the unknown coefficients $c_i$. Which leads via

$$\begin{aligned} \sum_i c_i \psi_1^p = \Gamma &= pu \\ &= \sum_i d_i p \psi_i \\ &= \sum_i d_i \psi_i^p. \end{aligned} \tag{10}$$

to a comparison of coefficients $d_i = c_i$ and from there to the desired solution $u$. The spectral combination is an inversion-free and stable method, but restricted to first and second order radial derivatives as observations. There is an extended literature about spectral modeling. Without attempting to be close to completeness the following newer references are to be mentioned: Freeden et al. (1999), Freeden and Hesse (2002), Freeden and Maier (2003), and Schmidt et al. (2005, 2006). Unfortunately, the spectral modeling is not directly applicable for along-track and out-of-plane gravity gradients. The idea to relate those observations to a localizing base function representation of the unknown potential is similar to the classical Lagrangian disturbing theory. There the observed orbital disturbances are expressed as linear combination of multi-periodic functions, weighted by the unknown coefficients of the spherical harmonics expansion of the potential. There are two differences between the classical Lagrangian disturbing theory and the development the paper is aiming at:

1. Instead of spherical harmonics here localizing base functions are to be used.
2. Instead of orbital disturbances gravity gradients in three orthogonal directions are used as observations.

The way this goal is to be achieved is similar to the classical Lagrangian disturbing theory: Transformation of the potential representation to a coordinate system, which follows the movement of the satellite cf. Sneeuw (1992).

## 3 Representation Theory of $SO(3)$

Both the definition of a system of localizing radial basis functions and the establishment of a relationship between such a representation and in-situ observations make use of the representation theory of $SO(3)$. For this purpose the necessary results from representation theory are to be compiled here.

The group of rotations of $\mathbb{R}^3$ around the origin is denoted by $SO(3)$. It consists of real 3-by-3 orthogonal matrices of determinant $+1$. To each $g = u(\gamma)a(\beta)u(\alpha) \in SO(3)$ an operator $\Lambda(g)$ acting on $L^2(\sigma)$ can be associated

$$(\Lambda(g)f)(\omega) := f(g^{-1}\omega), \tag{11}$$

with the matrices $a, u$ given by

$$a(\alpha) := \begin{bmatrix} \cos\alpha & 0 & -\sin\alpha \\ 0 & 1 & 0 \\ \sin\alpha & 0 & \cos\alpha \end{bmatrix} \tag{12}$$

and

$$u(\beta) := \begin{bmatrix} \cos\beta & \sin\beta & 0 \\ -\sin\beta & \cos\beta & 0 \\ 0 & 0 & 1 \end{bmatrix}. \tag{13}$$

Every rotated version $\Lambda(g)\bar{Y}_{nm}$ of a surface spherical harmonic is the following linear combination of the non-rotated surface spherical harmonics of the same degree:

$$\Lambda(g)\bar{Y}_{nm}(\vartheta,\lambda) = \sum_{k=-n}^{n} D(g)_{km}^n \bar{Y}_{nk}(\bar{\vartheta},\bar{\lambda}), \tag{14}$$

with

$$D_{km}^l(g) = e^{\imath k\alpha} d_{km}^l(\beta) e^{\imath m\gamma}, \tag{15}$$

where $\bar{\vartheta}, \vartheta$ and $\bar{\lambda}, \lambda$ are co-latitude and longitude in the non-rotated and the rotated system, respectively.

The functions $d_{km}^l(\beta)$ are called Wigner-d functions and are defined as follows

$$\begin{aligned} d_{km}^l(\beta) = (-1)^{m-k} &\sqrt{\frac{(l+m)!(l-m)!}{(l+k)!(l-k)!}} \\ &\times (\sin\frac{\beta}{2})^{m-k} (\cos\frac{\beta}{2})^{k+m} \\ &\times P_{l-m}^{(m-k,m+k)}(\cos\beta), \end{aligned} \tag{16}$$

with $P_l^{(m,n)}$ being the Jacobi Polynomials (Vilenkin 1968).

## 4 Transformation to Orbital System

Local gravity field representation means an approximation of the residual field by rotated versions of the radial base functions

$$\delta V(\omega) = \sum_{i=1}^{N} c_i \psi_i(\omega). \tag{17}$$

In order to determine the unknown coefficients $c_i$ and the unknown placements $g_1^{-1}\mathbf{e}_3$ in the radial base function representation of the residual field, the residual field has to be related to residual SST or gradiometry observations.

If a body-fixed coordinate system $x, y, z$ is attached to the satellite in such a way that $x$ points in radial, $y$ points in along track and $z$ points in out-of-plane direction (see Figure 2), only for the radial tensor component $\delta V_{xx}$ a simple relationship

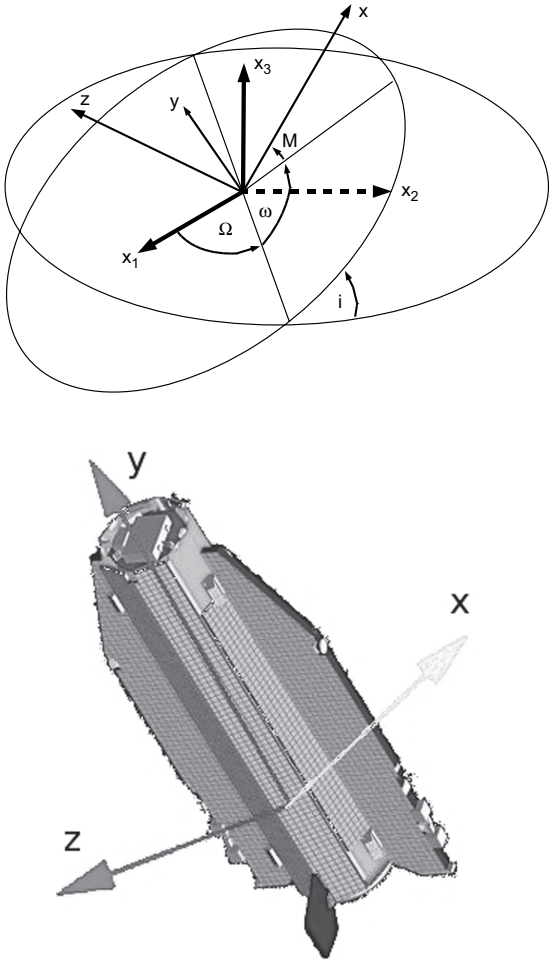


**Fig. 2.** Body-fixed coordinate system (bottom) and its relationship to the space-fixed system (top).

to the free parameters $c_i$ of the field representation is known. In what follows $SO(3)$ representation theory will be used to establish a similar relationship for the remaining two tensor components $\delta V_{yy}, \delta V_{zz}$. The relationship between the body-fixed and the space fixed system is approximatively given by the following rotation

$$g = u(\Omega - \Theta - \frac{\pi}{2})a(i)u(\frac{\pi}{2} + \omega + M) \tag{18}$$

where $\omega, \Omega, i, M$ are the mean elements of the orbital arc under consideration.

The representation of a radial base function in the rotating system is given by

$$\begin{aligned}(\Lambda(g)\psi_i)(\mathbf{x}) &= \Lambda(g)\sum_{n\in\mathbb{N}}\sigma_n\frac{2}{2n+1}\left(\frac{R}{\|\mathbf{x}\|}\right)^{n+1}\\ &\quad\sum_{m=-n}^{n} Y_{n,m}(g_i\mathbf{e}_3)Y^*_{n,m}(\frac{\mathbf{x}}{\|\mathbf{x}\|})\\ &= \sum_{n\in\mathbb{N}}\sigma_n\frac{2}{2n+1}\left(\frac{R}{\|\mathbf{x}\|}\right)^{n+1}\\ &\quad\sum_{m=-n}^{n} Y_{n,m}(g_i\mathbf{e}_3)\cdot\Lambda(g)Y^*_{n,m}(\frac{\mathbf{x}}{\|\mathbf{x}\|})\\ &= \sum_{n\in\mathbb{N}}\sigma_n\frac{2}{2n+1}\left(\frac{R}{\|\mathbf{x}\|}\right)^{n+1}\\ &\quad\sum_{m=-n}^{n} Y_{n,m}(g_i\mathbf{e}_3)\cdot Y^*_{n,m}(g^{-1}\bar{\omega}).\end{aligned}$$

Here, $\bar{\omega}$ is the position of the satellite in the rotating system.

Since for an exact circular orbit $\bar{\omega} = \mathbf{e}_1$ holds also for weakly eccentric orbits approximatively holds:

$$\begin{aligned}(\Lambda(g)\psi_i)(\mathbf{x}) &= \sum_{n\in\mathbb{N}}\sigma_n\frac{2}{2n+1}\left(\frac{R}{\|\mathbf{x}\|}\right)^{n+1}\\ &\quad\sum_{m=-n}^{n} Y_{n,m}(g_i\mathbf{e}_3)\cdot Y^*_{n,m}(g^{-1}\mathbf{e}_1)\\ &= \sum_{n\in\mathbb{N}}\sigma_n\left(\frac{R}{\|\mathbf{x}\|}\right)^{n+1} P_n((g_i\mathbf{e}_3\cdot(g^{-1}\mathbf{e}_1)).\end{aligned}$$

Besides this an equivalent representation of $(\Lambda(g)\psi_i)(\mathbf{x})$ is useful:

$$(\Lambda(g)\psi_i)(\mathbf{x}) = \sum_{n\in\mathbb{N}}\sigma_n\frac{2}{2n+1}\left(\frac{R}{\|\mathbf{x}\|}\right)^{n+1}$$

$$
\begin{aligned}
&\sum_{m=-n}^{n} Y_{n,m}(g_i\mathbf{e}_3)\cdot\Lambda(g)Y^*_{n,m}(\frac{\mathbf{x}}{\|\mathbf{x}\|})\\
&=\sum_{n\in\mathbb{N}}\sigma_n\frac{2}{2n+1}\left(\frac{R}{\|\mathbf{x}\|}\right)^{n+1}\\
&\quad\sum_{m=-n}^{n} Y_{n,m}(g_i\mathbf{e}_3)\cdot\Lambda(g)Y^*_{n,m}(\frac{\mathbf{x}}{\|\mathbf{x}\|})\\
&=\sum_{n\in\mathbb{N}}\sigma_n\frac{2}{2n+1}\left(\frac{R}{\|\mathbf{x}\|}\right)^{n+1}\\
&\quad\sum_{m=-n}^{n} Y_{n,m}(g_i\mathbf{e}_3)e^{\imath m(\frac{\pi}{2}+\omega+M)}\cdot\\
&\quad\sum_{k=-n}^{n} e^{\imath k(\Omega-\Theta-\frac{\pi}{2})}d^n_{m,k}(i)Y_{n,k}(\bar{\omega}).
\end{aligned}
$$

With the introduction of the abbreviations

$$
F_{n,m}(i,\Omega,\Theta):=\sum_{k=-n}^{n} e^{\imath[k(\Omega-\Theta-\frac{\pi}{2})]}d^n_{k,m}(i)Y_{n,k}(\bar{\omega}) \tag{19}
$$

and

$$
G_{n,m}(g_i,\omega,M):=Y_{n,m}(g_i\mathbf{e}_3)e^{\imath m(\frac{\pi}{2}+\omega+M)} \tag{20}
$$

this leads to the final result

$$
\begin{aligned}
(\Lambda(g)\psi_i)(\mathbf{x})=&\sum_{n\in\mathbb{N}}\sigma_n\frac{2}{2n+1}\left(\frac{R}{\|\mathbf{x}\|}\right)^{n+1}\\
&\sum_{m=-n}^{n} G_{n,m}(g_i,\omega,M)\times\\
&\times F_{n,m}(i,\Omega,\Theta)
\end{aligned} \tag{21}
$$

## 5 Observation Equations

The second order derivatives in

- $x$ -radial direction
- $y$ -along-track direction
- $z$ -across-track direction

are given by (see Koop 1993):

$$
\begin{aligned}
\frac{\partial^2\Lambda(g)\psi_i}{\partial x^2}&=\frac{\partial^2\Lambda(g)\delta V(\omega)}{\partial r^2}\\
&=\sum_{n\in\mathbb{N}}\sigma_n\left(\frac{R}{\|\mathbf{x}\|}\right)^{n+3}\\
&\quad\times\frac{(n+1)(n+2)}{R^2}\\
&\quad\times P_n(g_i\mathbf{e}_3\cdot(g^{-1}\mathbf{e}_1))
\end{aligned}
$$

$$
\begin{aligned}
\frac{\partial^2\Lambda(g)\psi_i}{\partial y^2}&=\frac{1}{a^2}\frac{\partial^2\Lambda(g)\delta V(\omega)}{\partial(M+\omega)^2}\\
&\quad+\frac{1}{a}\frac{\partial\Lambda(g)\delta V(\omega)}{\partial r}\\
&=\sum_{n\in\mathbb{N}}\sigma_n\frac{(n+1)}{Ra}\left(\frac{R}{\|\mathbf{x}\|}\right)^{n+2}\\
&\quad\times P_n(g_i\mathbf{e}_3)\\
&\quad-\sum_{n\in\mathbb{N}}\sigma_n\frac{2}{(2n+1)a^2}\left(\frac{R}{\|\mathbf{x}\|}\right)^{n+1}\\
&\quad\sum_{m=-n}^{n} m^2Y_{n,m}(g_i\mathbf{e}_3)Y_{n,m}(g\mathbf{e}_1)\\
\frac{\partial^2\Lambda(g)\psi_i}{\partial z^2}&=\frac{\partial^2\Lambda(g)\delta V(\omega)}{a^2\sin^2(M+\omega)\partial i^2}\\
&\quad+\frac{1}{a}\frac{\partial\Lambda(g)\delta V(\omega)}{\partial r}\\
&=\sum_{n\in\mathbb{N}}\sigma_n\frac{(n+1)}{Ra}\left(\frac{R}{\|\mathbf{x}\|}\right)^{n+2}\\
&\quad\times P_n(g_i\mathbf{e}_3)\\
&\quad+\frac{1}{a^2\sin^2(M+\omega)}\\
&\quad\sum_{n\in\mathbb{N}}\sigma_n\frac{2}{2n+1}\left(\frac{R}{\|\mathbf{x}\|}\right)^{n+1}\\
&\quad\sum_{m=-n}^{n}\times\\
&\quad G_{n,m}(g_i,\omega,M)\cdot\frac{\partial^2F_{n,m}(i,\Omega,\Theta)}{\partial i^2}
\end{aligned} \tag{22}
$$

Relations (22) establish the analytic relationships between the localizing base functions representation and gravity gradient observations in three orthogonal directions.

## 6 Numerical Example

In order to verify the derivations above, a simple forward computation was carried out. For a single GOCE arc the along track gravity-gradient tensor component $\delta V_{yy}$ was computed twice: Once by numerical orbit computation and once using the relations (22). As gravity field a three-basis functions regional model $\delta V$ on top of GGSM02 was used.

In order to relate the arc to the residual potential, a projection of the satellite ground track onto the residual potential is displayed in Figure 3. Along this track the quantities $\delta V_{yy}$ were computed both numerically and analytically. In Figure 4 the difference between the true gradiometry signal (i.e. the

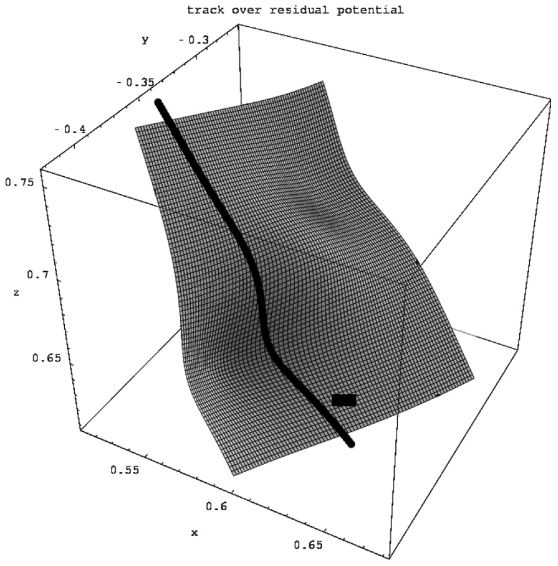


**Fig. 3.** Track over residual potential.

result of the numerical computation) and its analytical computation is shown. It is clearly visible that the numerical and the analytical solution match almost perfectly. This is an indication of the correctness of the obtained relationship between along-track in-situ observations and regional basis functions representation. For the test of the inverse computation, i.e. the recovery of the regional disturbing potential $\delta V$ from the observed along-track gravity gradients the same arc was used. Along the arc equidistantly 12 base functions were placed and the amplitudes of these base functions were estimated using the gravity gradient data along the arc. Figure 5 shows in the upper panel the difference between the true potential and the estimated potential. Since the gravity gradient is basically a second order derivative it is *blind*

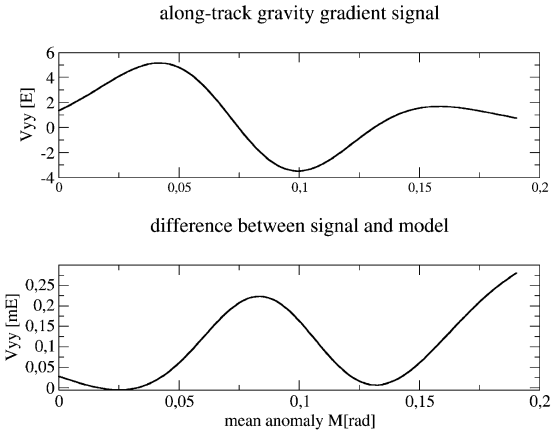


**Fig. 4.** Gradient signal (top) and difference between gradient signal and model (bottom).

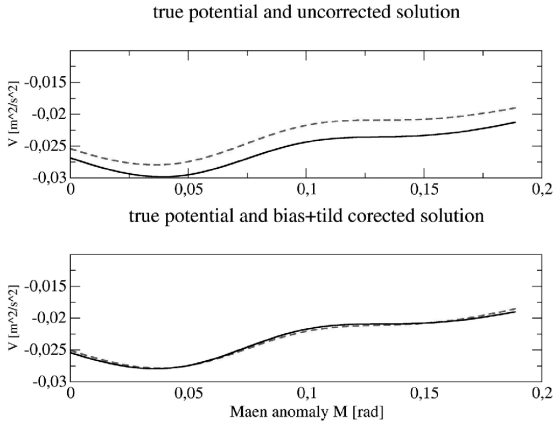


**Fig. 5.** Gradient signal (top) and difference between gradient signal and model (botton).

for bias and tilt. Therefore, the recovered potential differs from the true potential by a bias and a drift. After bias and drift removal the recovered potential almost perfectly matches the true potential.

## 7 Conclusions

A simple analytic relationship between in-situ observations of the Earth's gravity field and its representation by localizing base functions has been known only for radial gravity gradients observations. In the paper a similarly simple relationship also for two other gravity gradient components has been found: The along-track and the out-of-plane component. For the derivation of these relations the same techniques was used as in Lagrangian disturbing theory for the conversion of the spherical harmonics representation of the gravity field to orbital elements: The representation theorie of the rotation group $SO(3)$.

In a forward computation the derived analytic formulea were compared to gravity gradients obtained by numerical differentiation. Both results match almost perfectly.

For the inverse computation gravity gradients along a single arc were resolved by 12 equally spaced base functions along the ground-track of the satellite arc. The resolved potential along the arc differs from the true potential by a bias and a tilt. After bias and tild removal both data agree very well.

## References

Freeden, W., Glockner, O. and M. Thalhammer (1999) Multiscale Gravitational Field Recovery from GPS-Satellite-to-Satellite Trackin. Studia Geophysica et Geodaetica, **43**: 229–264.

Freeden W. and K. Hesse (2002) On the Multiscale Solution of Satellite Problems by Use of Locally Supported Kernel

Functions Corresponding to Equidistributed Data on Spherical Orbits. Studia Scientiarum Mathematicarum Hungarica, **39**:37–74.

Freeden W. and T. Maier (2003) SST-Regularisierung durch Multiresolutionstechniken auf der Basis von CHAMP-Daten. Allgemeine Vermessungs-Nachrichten (AVN) **110** :162–175.

Schmidt M., Fabert O. and C.K. Shum (2005) On the estimation of a multi resolution representation of the gravity field based on spherical harmonics and wavelets. Journal of Geodynamics **39**: 512–526.

Schmidt M., Han S.-C., Kusche J., Sanchez L. and C.K. Shum (2006) Regional high-resolution spatio-temporal gravity modeling from GRACE data using spherical wavelets. Geophysical Research Letters, **33** L08403, doi:10.1029/2005GL025509.

Sneeuw N. (1992) Representation Coefficients and their Use in Satellite Geodesy, Manuscr. Geod. **17**:117–123.

Vilenkin N.J. (1968) *Special functions and the theory of group representations*, American Mathematical Society, Translations of Mathematical Monographs, Vol. 22.

Koop R. (1993) Global gravity modelling using satellite gravity gradiometry, Netherlands Geodetic Commission, Publications on Geodesy No 38, Delft 1993

Keller W. and M. Sharifi (2005) Satellite gradiometry using a satellite pair. Journal of Geodesy **78**: 544–557.

http://www.springer.com/978-3-540-74583-9

VI Hotine-Marussi Symposium on Theoretical and Computational Geodesy
IAG Symposium Wuhan, China 29 May - 2 June, 2006
Xu, P.; Liu, J.; Dermanis, A. (Eds.)
2008, XVII, 362 p., Hardcover
ISBN: 978-3-540-74583-9